The Applicability of Coulomb's Friction Law to Drawbeads in Sheet Metal Forming

HARMON D. NINE

During sheet metal forming on a double-action toggle press, drawbeads on the die binder supply a restraining force which controls the flow of sheet metal into the die. To study the restraining force and the related binder hold-down force, an apparatus was built which simulates a drawbead. The apparatus can separate the restraining force into its bending deformation and friction components. From experimental measurements of the appropriate forces a coefficient of friction for drawbeads may be obtained. A comparison of experimental and calculated friction forces shows that Coulomb's Law (a constant coefficient of friction) satisfactorily represents the friction force in low and medium load ranges. However, Coulomb's Law breaks down at higher loads. The load at which breakdown occurs depends on interactions among many variables including sheet metal material, lubricant, and surface roughness.

INTRODUCTION

In double-action toggle press forming of sheet metal, the first action lowers the binder (or blank holder) onto the periphery of the sheet to hold it in position, Figure 1(a). The second action lowers the punch, which draws the sheet metal into the die cavity. During the drawing of the sheet metal, the binder controls the flow of metal into the die to insure a successful stamping. Too much metal flow into the die cavity will produce wrinkling or poor part shape, while too little flow will cause tearing.

HARMON D. NINE is with the Physics Department, General Motors Research Laboratories, Warren, MI 48090.

This and the preceeding paper in this volume on drawbead forces are based on work done in a cooperative program among the General Motors Mathematics and Physics Departments of the Research Laboratories and Fisher Body Division. A previously published paper, "Drawbead Forces in Sheet Metal Forming,"[1] described experimental work on deformation and Coulomb's friction forces. The preceding paper of this set describes an analytical model and results of calculations for deformation and friction forces in drawbeads. This paper gives an expanded experimental study of friction forces extending work to loads where Coulomb's friction law breaks down. The three papers together give a comprehensive view of the experimental and analytical work on drawbead forces.

In some applications the proper amount of metal flow may be achieved by varying the hold-down force of a flat binder against the sheet metal to alter the friction force between the binder and the sheet metal as shown in Figure 1. For other applications, particularly large irregularly shaped parts, friction alone does not supply adequate restraining force for control, and drawbeads must be added to the binder. A drawbead is shown schematically in Figure 1(a) (inset) as a semicylindrical bead attached to one binder face. The drawbead fits into a groove on the opposing binder face. The drawbead creates extra restraining force by requiring the sheet metal to bend around the bead as it is drawn through the binder, thereby adding deformation to the friction force.

The bending deformation force and the material properties which influence the mathematical modeling of the deformation force were previously discussed in detail.[1] In that earlier study it was found that friction forces could be expressed by Coulomb's Law (constant coefficient of friction) over a certain range of experimental conditions. Subsequent work has shown, however, that Coulomb's Law breaks down beyond the initial range investigated. This paper cov-

ISSN 0162-9700/82/0706-00200$00.75/0

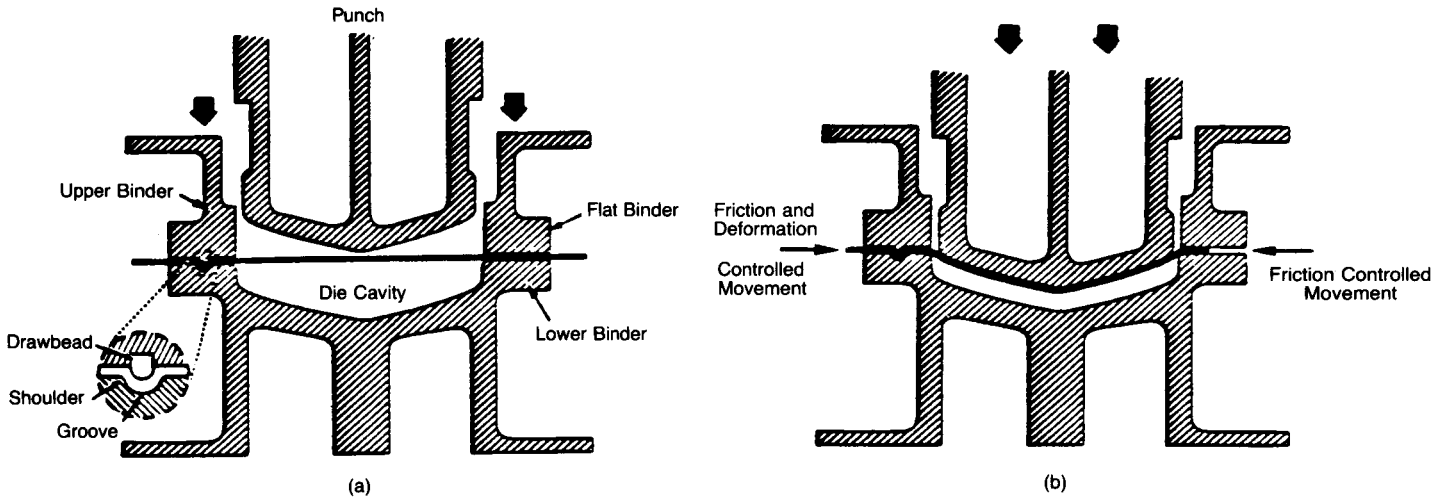

Fig. 1 — Double-action toggle press. (*a*) Action 1 — the binder moves down to hold the sheet metal in position for forming. (*b*) Action 2 — the punch moves down into the die cavity drawing sheet metal through the binders into the die cavity.

ers a broader range of friction conditions and determines where Coulomb's Law is applicable to the analysis and calculation of the friction force in drawbeads.

Drawbead Friction

The friction conditions in metal forming operations may be categorized into four regimes as described by Wilson:[2] (1) thick film, (2) thin film, (3) mixed, and (4) boundary. Which of these regimes is operable depends on such factors as lubricant, load, surface roughness, and deformation speed. Large changes in a coefficient of friction would be expected if the lubrication regime changed during a forming operation. Experiments were devised in this study to determine whether Coulomb's Law can characterize the friction for drawbeads under realistic production conditions.

For Coulomb's Law to apply, it is necessary that the real area of contact between the sheet metal and the drawbead surfaces be a linear function of the normal load. For thin film, mixed or boundary regimes, metal surfaces sliding over one another contact at high points on the surfaces called asperities. If loads are such that the contact between the asperities is plastic, and tangential loading does not effect the deformation, the fraction of the surface area in actual contact, a, will be a linear function of the normal load, P. Clean surfaces will weld at the asperity contacts and the mean friction shear stress, $\bar{\tau}_f$, will be,

$$\bar{\tau}_f = a\,\tau_s$$

where τ_s is the shear stress of the softer material. If a is a linear function of P, then

$$\bar{\tau}_f = \mu P$$

where μ is a constant coefficient of friction. This expression is simply a statement of Coulomb's Law of friction. However, at higher loads, tangential loading may cause an increase in the area of contact. Tabor[3] has proposed a junction growth model which allows the contact area at asperities to grow rapidly under the combined shear and normal forces. This would increase the ratio of the sliding shear force to the normal force, so that Coulomb's Law would no longer be applicable.

It would be extremely difficult to measure the true contact area of the surface asperities with the precision necessary to determine whether contact area was increasing linearly with normal force. Therefore, an expression for the coefficient of friction was derived in terms of measurable forces to determine whether μ stayed constant under increasing normal force. There are two measurable forces for drawbeads: (1) the drawbead restraining (DR) force, and (2) the binder hold-down (BH) force, Figure 2. The DR force is the force necessary to pull the sheet metal through the beads, and it

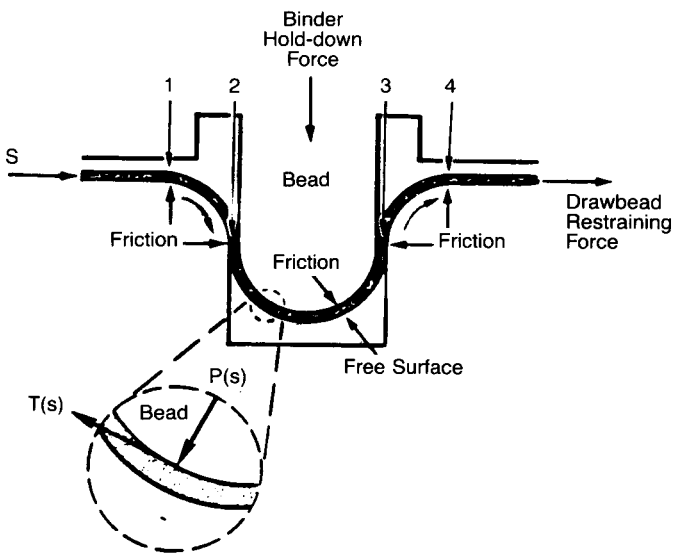

Fig. 2 — Schematic drawing of drawbead showing development of relevant forces.

controls the metal flow into the die. The BH force is the force required to hold the bead at a fixed penetration (or depth) between the shoulders of the bead groove.

A detailed analysis of drawbead forces is given in Reference 1 and is briefly presented here. Figure 2 traces the development of the forces on an area element as it passes through the drawbeads. Assuming a small clearance is maintained between the drawbead and the sheet, no forces are exerted prior to position 1. At position 1 the drawbead forces the metal to bend to the curvature of the first shoulder radius. All bending is done at position 1, thereby generating a small restraining force. No further bending occurs between 1 and 2 but the sheet metal is pressed against the shoulder by the deformation force at 1, which acts as a back force, in combination with the forward force supplied by the punch as the sheet metal is drawn into the die. The pressure of the sheet normal to the shoulder surface is proportional to the magnitude of the back force. This pressure in turn produces a friction restraining force.

Further bending occurs at positions 2, 3, and 4, which increases the deformation restraining force. Between positions 2 and 3, and 3 and 4, friction again increases the restraining force. Each increase in the restraining force from either deformation or friction acts as an additional back force for all locations closer to the bead exit. Therefore, the friction force continually increases toward the drawbead exit because the back force continually increases. The sum of all the individual friction and bending forces resolved along the sheet metal flow direction equals the measured drawbead restraining force. The sum of all the deformation and friction forces exerted on the binder, resolved in the vertical direction, Figure 2, is the binder hold-down force.

For drawbead friction, the following expression was derived in Reference 1 to obtain the coefficient of friction from measurements of DR and BH forces.

$$\mu = \frac{\tau(s)}{P(s)} = \frac{DR_{d+f} - DR_d}{\pi\, BH_{d+f}} = \frac{DR_f}{\pi\, BH_{d+f}} \qquad [1]$$

where

$\tau(s)$ = the sliding shear force as a function of position in the drawbead,

$P(s)$ = the force normal to the drawbead surface as a function of position in the drawbead,

DR_{d+f} = measured drawbead restraining force for fixed drawbeads,

DR_d = measured drawbead restraining force for "frictionless" drawbeads,

DR_f = drawbead restraining force due to friction only,

and BH_{d+f} = measured binder hold-down force for fixed drawbeads.

This expression is based on the assumption that the normal pressure, $P(s)$, remains constant through the drawbead.

From the foregoing discussion it is clear that the pressure does not remain constant, but increases through the drawbead. However, this simplifying assumption does not negate Eq. [1] if Coulomb's Law applies because then μ remains single valued at all points within the drawbead even though the pressure changes. A membrane approximation, which gives an exponentially increasing pressure distribution, is not strictly applicable since the sheet thickness is not small relative to the bending radius. Because bending forces are important, the sheet metal does not conform to the bead surface but skips contact at certain locations as may be observed by wear patterns. Thus, the actual pressure distribution in the drawbead is extremely complex. Nevertheless, the measured binder hold-down force is the resolved integrated average force which can be used in Eq. [1].

As a check on the effect of pressure distribution, a second expression, assuming a linearly increasing pressure distribution (more like the actual distribution) was derived.[1] Since this expression gave μ's approximately the same as Eq. [1], calculations in this study are based on the simpler Eq. [1].

EXPERIMENT

To achieve quantitative results it was necessary to separate the friction force from the deformation force. Experimentally this was accomplished with a "frictionless" drawbead in which the shoulders of the groove and the bead were replaced by rollers, Figures 3(a) and (b). These rollers are supported by sets of ball bearings. Since the surfaces of the rollers are free to rotate with the sheet metal, there is no sliding friction. The system is not, of course, completely frictionless since a small force is needed to overcome the friction of the rollers and the backing bearings. The coefficient of friction of ball bearings is about 0.001 to 0.002, depending on the lubrication conditions, which is negligibly small compared to that for regular beads.

The roller drawbeads were built to the same dimensions as sets of fixed drawbeads, shown in Figure 3(c), that simulate production drawbeads. The fixed drawbeads are made of production drawbead material, W-2 water-hardening steel, and are replaceable in case of excessive wear.

The support pieces which hold each drawbead set were designed so that the clearance between the shoulders can be adjusted by shims. This makes it possible to adjust for a constant, tight clearance while testing sheet metal of different thickness. In addition, guide rollers (Figure 3) are provided which hold the incoming sheet metal strips in the original plane of entry as the bead penetrates the groove shoulders. The positioning guides and clearance adjustments are necessary to obtain a well-defined geometry for experimental reproducibility and mathematical analysis. The drawbeads are mounted in an apparatus, Figure 4, which simulates the action of a press. The binder is represented by an hydraulic ram which drives the bead between

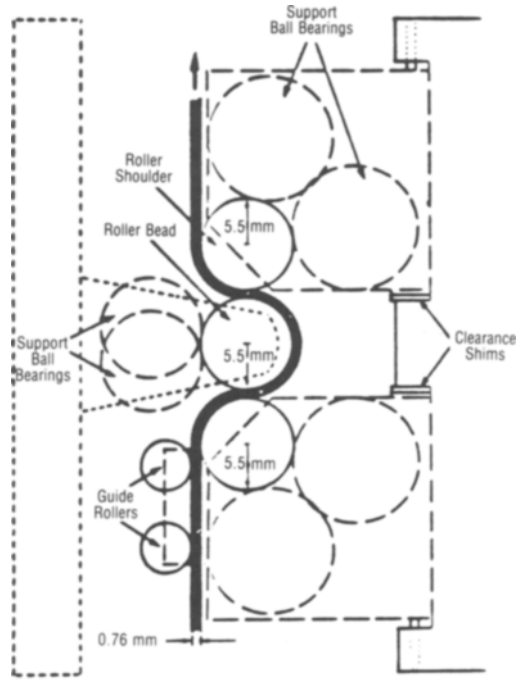

a.

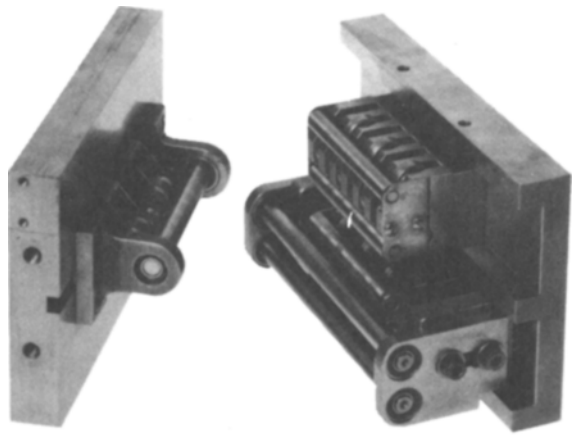

b.

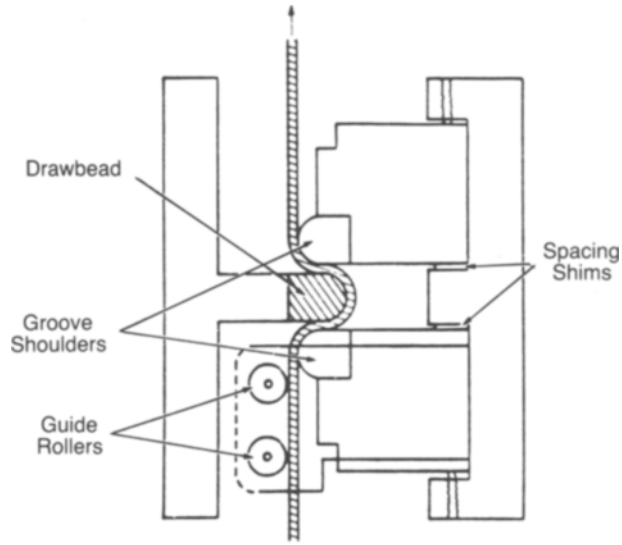

c.

Fig. 3—(*a*) Schematic drawing of roller drawbead fixture, (*b*) roller drawbead fixture, (*c*) fixed drawbead fixture.

the shoulders until the centers of radii of the bead and shoulders are aligned, as measured by a dial indicator. The sheet metal is drawn through the drawbeads by a grip to simulate the action of the punch. Load cells, shown in Figure 4, measure the DR and BH forces.

Sheet metal test strips were cut 400 mm long in the sheet rolling direction by 50 mm wide. The strips are inserted between the bead and shoulders, aligned vertically, and clamped in the grips. They are pulled through the drawbeads for a distance of 125 mm at a rate of 85 mm per second. This is the estimated average speed at which metal is drawn in production presses. Load *vs* stroke for both DR and BH loads are read from two-channel *x-y* recorder traces after the loads reach a steady state. All results are the average of at least three separate tests.

Drawbead forces were measured for drawbeads of two different bead and shoulder radii, 5.5 mm and 4.75 mm. By measuring forces for different thicknesses of sheet metal on these two drawbeads, a range of forces was obtained. The range of drawbead forces was somewhat limited because roller drawbeads with radii less than 4.75 mm failed under the higher loads imposed by the smaller radii. For the

thickest steels, 0.96 mm AK and 0.99 mm rimmed, the "frictionless" forces could not be measured, even for the 4.75 mm radius drawbeads, because of bearing failure.

The materials investigated were aluminum-killed (A-K) steel, rimmed steel, 2036-T4 aluminum, and 5182-0 aluminum. Table I lists the materials and their properties as determined in tensile tests. In the usual manner k and n were obtained from the true stress-true strain plots assuming power law strain hardening. The normal anisotropy parameter, $\bar{r}$, was obtained by measuring the change in shape of photogridded circles on uniformly strained tensile samples.

For each sheet material, various thicknesses (Tables II and III) were investigated. For the ~1 mm 2036-T4 aluminum, the first specimens evaluated displayed a large increase in μ compared to the thinner samples. Therefore, a second lot of material was tested. The second lot showed a μ much closer to the thinner samples. These two lots were designated LF and HF in Table III for low and high friction, respectively. Additional tests were performed on the LF and HF aluminum which included ESCA (Electron Spectroscopy for Chemical Analysis), Electron micro-probe examination, and profilometer traces to give AA (Arithmetic Average) surface roughness. These two lots were also buffed to impart the same surface to both samples.

Widely different lubrication conditions were investigated for all the materials to give a wide range of μ. The lowest values of μ were obtained with a proprietary soap base (SB) lubricant of good lubricity, while a mill oil (MO) lubricant with poor lubrication properties gave relatively high μ's. Typical DR and BH loads *vs* stroke, Figure 5, show the

Table I. Mechanical Properties of Test Materials

	K*	n*	$\bar{r}$*
Rimmed Steel	551 MPa	0.20	1.1
A-K Steel	516 MPa	0.23	1.6
2036-T4 Aluminum	643 MPa	0.25	0.68
5182-0 Aluminum	506 MPa	0.29	0.63

*Tabulated values are averages over the plane of the sheet obtained by using the form: $x_{average} = X_{0°} + 2X_{45°} + X_{90°}/4$ where 0°, 45°, and 90° refer to the strain direction relative to the sheet rolling direction of the material. Values for different thickness sheets of the same material were averaged.

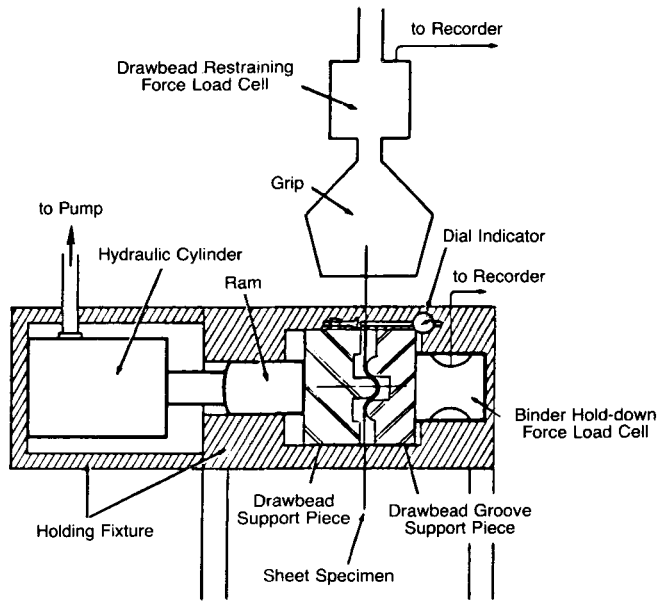

Fig. 4—Schematic diagram of drawbead simulator apparatus for measuring drawing and clamping forces.

Table II. Drawbead Forces and Coefficient of Friction for Test Lubricants on Steel

Lubrication Condition	Force or μ	Sheet Thickness mm	Rimmed Steel 0.76	Rimmed Steel 0.86	Rimmed Steel 0.99	AK Steel 0.76	AK Steel 0.86	AK Steel 0.96	
MO Lubricant	DR (kN)		5.7	6.4	8.4	5.6	6.4	8.0	
	BH (kN)		4.2	4.8	5.8	4.2	4.8	5.9	
	μ		0.18	0.16	0.17	0.18	0.16	0.16	
Rollers	DR (kN)		3.3	3.9	5.3	3.3	3.9	5.0	5.5 mm radius drawbead
	BH (kN)		3.0	3.5	4.7	2.7	3.2	4.0	
SB Lubricant	DR (kN)		4.0	4.8	6.3	4.0	4.6	6.0	
	BH (kN)		3.4	4.2	5.2	3.4	4.1	5.0	
	μ		0.07	0.07	0.06	0.07	0.05	0.06	
MO Lubricant	DR (kN)		6.3	9.1	*	5.7	6.9	*	
	BH (kN)		4.7	6.6		4.2	4.9		
	μ		0.17	0.18		0.16	0.16		
Rollers	DR (kN)		3.8	5.4		3.6	4.3		4.75 mm radius drawbead
	BH (kN)		3.4	4.6		3.3	3.7		
SB Lubricant	DR (kN)		4.6	7.2		4.5	5.3		
	BH (kN)		3.9	5.5		3.8	4.1		
	μ		0.06	0.11		0.07	0.07		

*These forces were not measured because they exceeded the capacity of the apparatus.

Table III. Drawbead Forces and Coefficient of Friction from Test Lubricants on Aluminum

Lubrication Condition	Force or μ	Sheet Thickness (mm)	2036-T4 Aluminum 0.81	0.89	*LF 0.97	**HF 0.99		5182-0 Aluminum 0.82	0.99	
MO Lubricant	DR (kN)		4.7	5.7	6.1	7.0		3.3	5.0	
	BH (kN)		3.6	4.8	4.9	4.9		2.6	2.8	
	μ		0.18	0.17	0.16	0.21		0.18	0.22	
Rollers	DR (kN)		2.8	3.2	3.7	3.8		1.9	3.1	5.5 mm radius
	BH (kN)		2.2	2.8	3.2	3.1		1.7	2.1	drawbead
SB Lubricant	DR (kN)		3.0	3.9	4.4	4.5		2.5	3.5	
	BH (kN)		2.9	3.5	4.1	3.8		2.2	3.0	
	μ		0.04	0.07	0.06	0.06		0.09	0.05	
MO Lubricant	DR (kN)		4.8	5.9	6.9	8.5	7.3†	4.0	5.8	
	BH (kN)		3.8	4.7	4.5	4.6	4.6†	2.6	4.1	
	μ		0.17	0.14	0.19	0.27	0.18†	0.21	0.19	
Rollers	DR (kN)		2.9	3.8	4.3	4.6		2.3	3.4	4.75 mm radius
	BH (kN)		2.3	2.8	3.4	3.5		1.8	2.9	drawbead
SB Lubricant	DR (kN)		3.8	4.9	5.1	5.8		2.7	4.1	
	BH (kN)		2.9	4.2	4.3	4.9		2.2	3.4	
	μ		0.10	0.08	0.06	0.08		0.07	0.06	
No Lubricant	DR (kN)				8.3	***				
	BH (kN)				3.1					
	μ				0.42					

*LF = low friction lot
**HF = high friction lot
***Sheet metal galled and seized
†0.99 2036-T4 Al–forces measured after buffing

large differences between these lubricants for 0.86 mm AK steel with 11 mm diameter drawbeads.

RESULTS AND DISCUSSION

The DR and BH loads for different thicknesses of the materials investigated are shown for the two different drawbead diameters in Tables II and III. Coefficients of friction, obtained from Eq. [1], are also shown in the tables. For the MO lubricant, the friction force lies between 36 pct and 46 pct of the total drawbead force, while for the SB lubricant the friction force is only between 13 pct and 21 pct of the total drawing force.

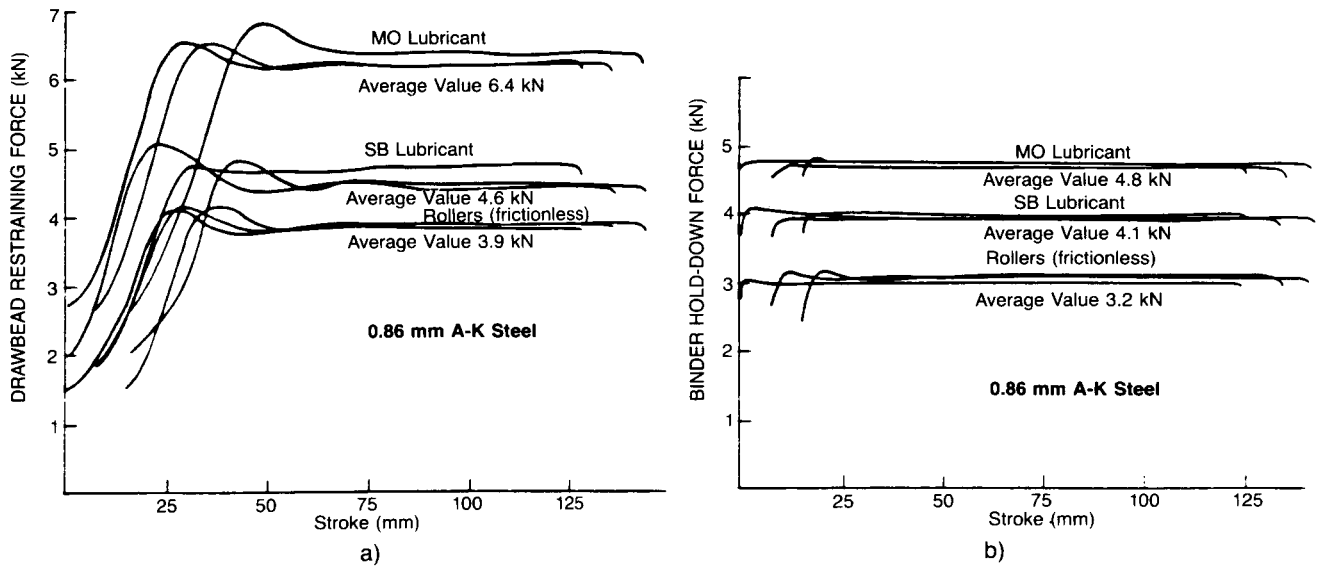

Fig. 5—Force *vs* stroke measurements for drawbead forces in 11 mm diameter "frictionless" and fixed drawbeads for 0.86 mm AK steel. Mil oil and soap base lubricants were measured for the fixed drawbead. (*a*) DR (Drawbead Restraining) force, (*b*) BH (Binder Hold-down) force.

The scatter in μ values is greater for the SB lubricant than for the MO lubricant, but this does not imply a less accurate measurement. Since μ depends directly on the difference between the restraining forces from standard drawbeads (DR_{d+f}) and the roller beads (DR_d), the percent error in the calculated μ increases as the average Dr_{d+f} approaches DR_d, *i.e.*, as the lubricant improves.

Steels

The relatively constant behavior of μ for two specific lubricants as the BH force is varied by changing steel thickness and drawbead diameter is shown in Table II. For the MO lubricant μ varied between 0.16 and 0.18, a range of about 12 pct, while the BH force varied from 4.2 kN to 6.6 kN, a range of over 50 pct. Similarly the coefficient of friction for the SB lubricant for most steel strips varied between 0.05 and 0.07 (about 20 pct), while the BH force varied from 3.4 kN to 5.2 kN (over 50 pct). These relatively small changes in μ for a large variation in BH force is an indication that Coulomb's Law can reasonably represent friction for these cases.

In contrast to the Coulombic behavior of μ discussed above, the 0.86 mm thick rimmed steel showed an increase in μ to 0.11 for measurements on the 4.75 mm radius drawbead, compared to the 0.05 to 0.07 range noted for the other steel measurements. This departure was accompanied by burnishing of the bead and shoulders of the drawbead, demonstrating that the lubricant was not effectively preventing metal to metal contact. Apparently the lubricant had shifted from a thin film regime to a mixed lubrication regime. Values of μ for the thicker steel, about 1 mm thickness, could not be obtained for the 4.75 mm radius drawbeads because the forces exceeded the load capability of the roller bead apparatus.

Aluminum Alloys

The coefficients of friction, Table III, for the MO lubricant on 0.81 mm and 0.89 mm thick 2036-T4 aluminum are similar to those for the steels. Since 2036-T4 aluminum sheet is designed to have yield characteristics similar to steel, the similarity of μ to that of steel for a given lubricant is reasonable. However, μ for 0.99 mm thick 2036-T4 aluminum, measured on the 4.75 mm radius drawbead with MO lubricant, increased to 0.27 compared to 0.16 for the two thinner test strips, an increase of over 50 pct. This large change in μ indicates a departure from Coulomb's Law, *i.e.*, the coefficient of friction is no longer constant.

In order to determine the cause of the change in μ, a second lot of 2036-T4 aluminum of about the same thickness was tested under the same conditions. μ for this lot of material was 0.19, much closer to μ's previously found. As noted in the experimental section, the two lots of material were designated LF (low friction) and HF (high friction). Surface analysis by ESCA and electron microprobe showed no significant differences in trace elements or oxides. However, surface roughness, as measured an AA, was significantly different between LF and HF aluminum. The LF material measured an AA roughness of 0.05 μm along the sample length (sheet rolling direction) and 0.27 μm across the sample (transverse to sheet rolling direction). The HF material measured an AA roughness of 0.11 μm along the rolling direction and 0.56 μm transverse to the rolling direction. While much more sophisticated means of measuring surface roughness are necessary to fully characterize the surfaces in terms of true contact area,[4] these methods are beyond the scope of the current work. The AA measurement does give at least a first indication of surface roughness. Figure 6 shows SEM photomicrographs and associated AA roughness measurements for an HF sample. By buffing the HF sample, its AA roughness was reduced to about 0.08 μm in both sheet directions. After buffing, μ for the HF sample decreased to 0.18 for MO lubricant on the 9.5 mm diameter drawbead, which approximates μ for the LF material. The similarity of μ for the LF and HF aluminum after buffing shows that surface roughness is a decisive factor in the friction differences between the two lots with MO lubricant. Note, however, from Table III that no significant differences in friction between LF and HF samples are observed for the SB lubricant. This is believed to be related to the lubrication regime. At the measured BH loads the aluminum strips probably operate in the mixed lubrication regime with MO lubricant, but in the thin film regime for SB lubricant. The interaction between lubricants and surface roughness in sheet metal drawing has been reported in the literature.[5,6]

In drawbeads the relation between the surface roughness and friction is particularly complex because the surface roughness changes as the sheet metal progresses through the drawbead. If sheet metal is deformed in contact with a die surface, the sheet surfaces become smoother. However, if the sheet metal is deformed as a free surface, the sheet becomes rougher.[7] Both types of deformation are experienced by both surfaces of the sheet as it traverses a drawbead and is alternately bent against the bead and the shoulders. Variations in the surface roughness of the HF aluminum as the metal progresses through the 4.75 mm drawbead can be readily observed, Figure 6.

From both the SEM micrographs and the AA roughness measurements it is evident that the metal surface is flattened more by contact with the second shoulder than with the first. This indicates an increase in the normal contact pressure as the strip progresses through the drawbead. Since Coulomb's Law will apply to friction in drawbeads only as long as the true contact area is a linear function of the normal pressure, the severe flattening at the second shoulder, a reduction in

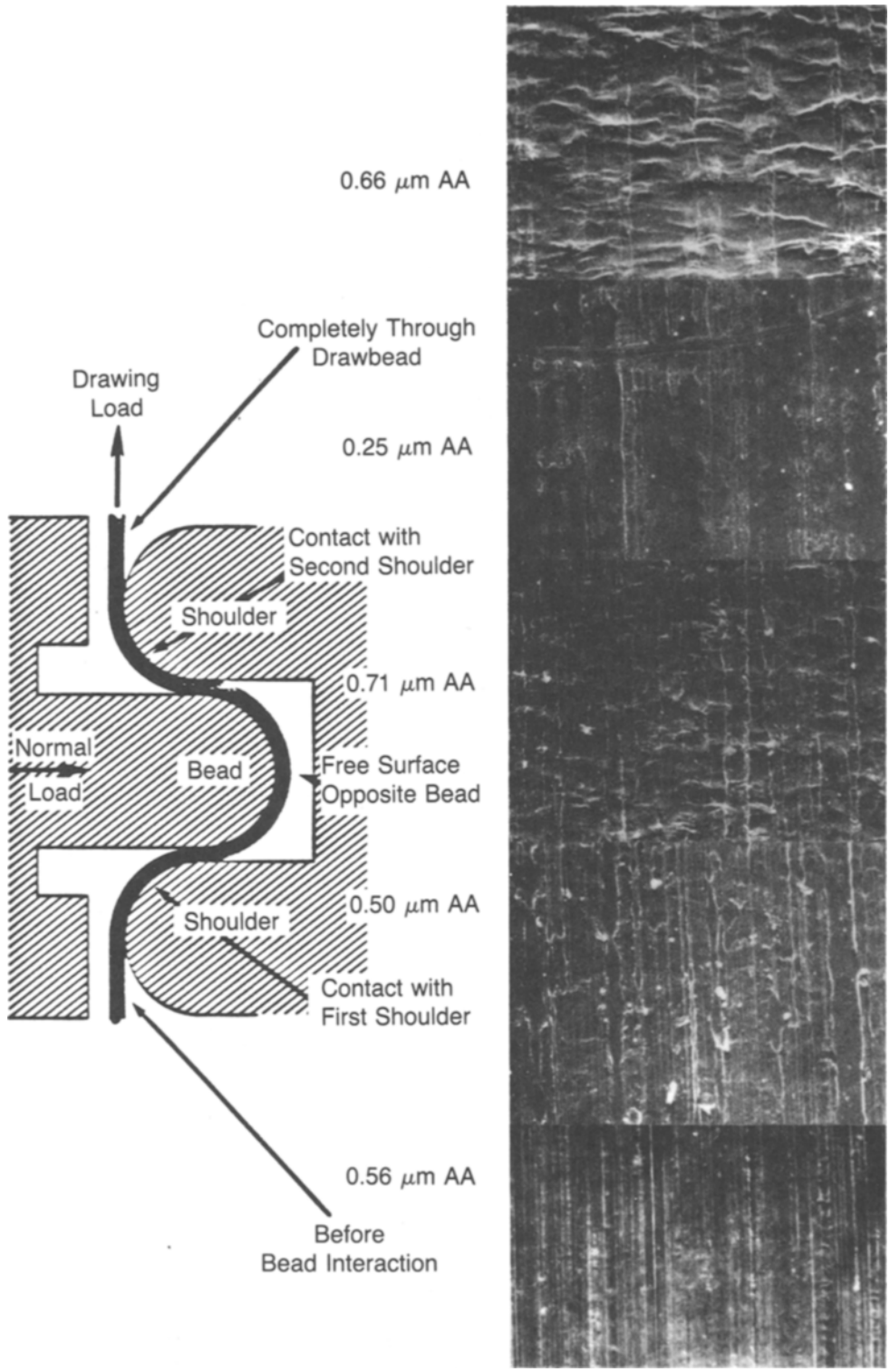

Fig. 6—The variation of surface roughness with position in the 4.75 mm radius drawbead for 0.99 mm thick 2036-T4 (HF) aluminum shown by SEM micrographs and profilometer measurements transverse to the rolling direction.

roughness from 0.71 μm AA to 0.25 μm AA shown in Figure 6, suggests a departure from Coulomb's Law.

The departure from Coulomb's Law can also be noted by a plot of DR force vs BH force for the MO lubricant, Figure 7. Over most of its range, the plot shows a linear relationship between DR and BH forces as expected from Coulomb's Law. The value of μ over this range is ~0.17 from Table II. However, a sharp departure from linearity is observed at a BH force of about 4.6 kN. At this force, μ suddenly increases to over 0.21. The high DR force data points are for 0.97 mm LF aluminum on 9.5 mm diameter beads and 0.99 mm HF aluminum on both 9.5 mm and 11 mm diameter drawbeads, as shown in Table III.

5182-O aluminum shows a somewhat higher μ (Table III) than 2036-T4 for comparable BH forces with the MO lubricant. This alloy is softer than 2036-T4 aluminum, so that the

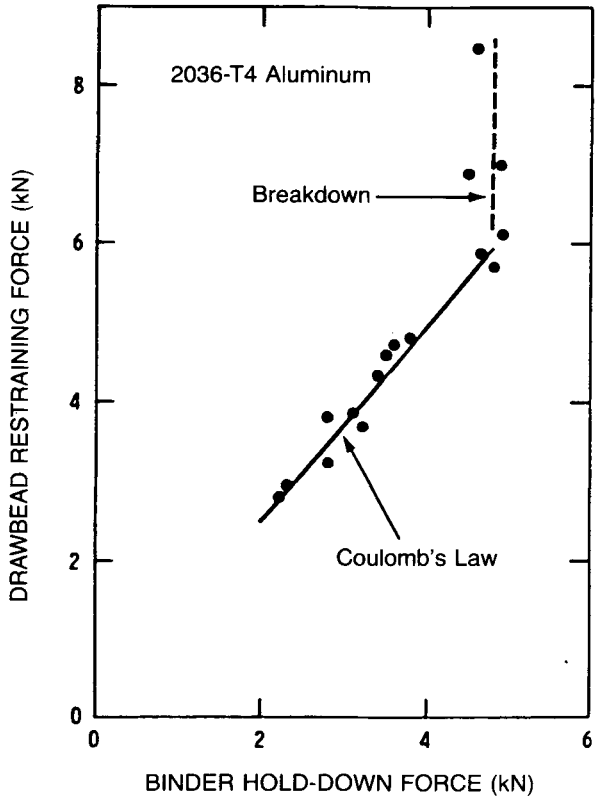

Fig. 7—Drawbead Restraining force *vs* Binder Hold-down force for 2036-T4 aluminum.

true area of contact would be larger for a given BH force. Therefore the coefficient of friction would be expected to be higher. No departure from Coulomb's Law was observed for 5182-O aluminum, but BH forces were relatively low because of the lower strength of this alloy. The coefficient of friction for the SB lubricant on 5182-0 aluminum is about the same as for 2036-T4 aluminum. This again indicates that the SB lubricant operates in the thin film region where the lubricant is more important than the sheet metal characteristics.

Comparison of Analytical and Experimental Drawbead Restraining Forces

Wang[8] has analyzed drawbead forces and calculated the drawbead restraining force based on bending deformation and friction. His deformation force analysis incorporates the relevant material properties and assumes that the material strain hardens monotonically. The friction force calculation assumes Coulomb's Law. Since friction is assumed to be Coulombic for Wang's model, a test of the applicability of Coulomb's Law to drawbeads is provided by comparing Wang's calculated values of DR force plotted for assumed μ's to experimental DR force values plotted for μ's obtained from Eq. [1].

Figure 8 shows that for 0.89 mm 2030-T4 aluminum and 0.86 mm A-K steel pulled through 4.75 mm radius drawbeads the experimental curves of DR force *vs* μ closely parallel the curves calculated by Wang. The difference in magnitude between the experimental and calculated curve for aluminum probably occurs because Wang's analysis of deformation force assumes monotonic strain hardening rather than cyclic strain hardening. Cyclic strain hardening would cause less hardening, but the magnitude is not known. However, since experimental and calculated curves maintain a nearly constant separation as μ increases from zero, there is good agreement for the friction part of the DR force. The large difference in the deformation component of DR force is not found for steel because steel has a strain-rate hardening effect not present in aluminum. The increased hardening due to the strain rate effect in steel is about 20 pct for drawbead deformation conditions.[1] The cyclic softening effect for aluminum based on Figure 8 is about 20 pct. Since neither effect is included in Wang's analysis,[4,8] the good agreement between experiment and calculation for steel may result from a cancelling of these two effects.

For the thickest steels (0.99 mm rimmed and 0.96 A-K) in 5.5 mm radius drawbeads, and for the two thinnest 2036-T4 aluminum specimens on 4.75 mm radius drawbeads, there was also good agreement between calculated and experimental values. The upward curvature of Figure 8

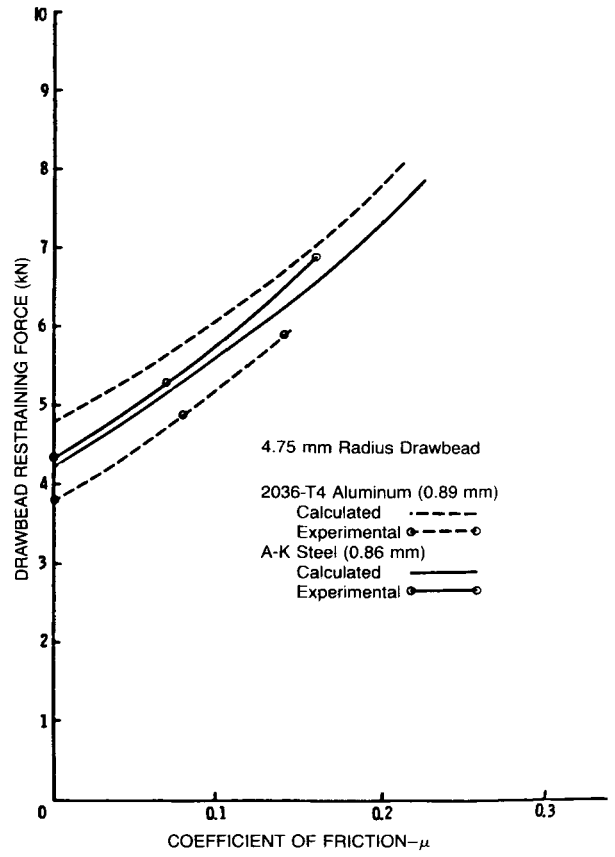

Fig. 8—Drawbead Restraining force *vs* μ for 0.86 mm A-K steel and 0.89 mm 2036-T4 aluminum on 4.75 mm radius drawbeads. Calculated and experimental curves are nearly parallel, showing that Coulomb's Law is a reasonable approximation for these cases.

is a result of the complex interplay between friction and DR force due to the drawbead geometry as discussed earlier. Thus, for these sheet metals and operating conditions, Coulomb's Law gives a good representation of the friction component of the DR force.

However, for the thick aluminum on the 5.5 mm radius drawbead, some deviation from Coulomb's Law is observed. Figure 9 shows that the HF aluminum begins to deviate slightly toward lower drawing force with increasing μ compared with the calculated curve. The difference between the calculated the experimental curve for the HF aluminum increases from about 1 kN at zero friction to 1.4 kN for friction with MO lubricant, while the difference between calculated and experimental curves for LF aluminum remains constant at ~1.6 kN for the same two conditions.

Much greater deviations between the calculated and measured DR forces develop for aluminum pulled through the 4.75 mm radius drawbead because of increased contact pressure between the sheet metal and drawbead. The experimental values of DR force continually decrease below the calculated values as μ increases for both LF and HF 2036-T4 aluminum. The difference between calculated and experimental DR force increases from 1.7 kN for the LF aluminum at zero friction to 2.5 kN at μ = 0.19 for MO lubricant. The HF aluminum shows a greater difference from 1.2 kN at zero friction to 3.2 kN at μ = 0.27 for the MO lubricant. For no lubricant (dry), μ equals 0.42 and the DR force for the LF aluminum drops far below the calculated curve based on Coulomb friction. The dry point for the HF aluminum could not be obtained because the friction force was so high that the sample failed in tension. Both the LF and HF aluminum galled for the dry cases, which indicates a complete change of lubrication regime. It is clear from Figure 10 that for poor lubrication conditions under the higher contact loads imposed by smaller radius drawbeads and/or thicker specimens, Coulomb's Law breaks down for

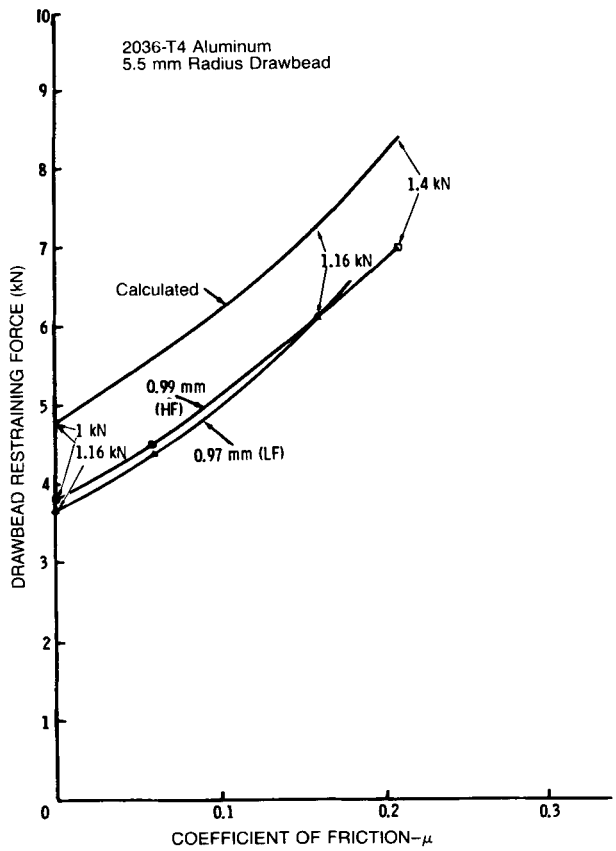

Fig. 9 — Drawbead Restraining force *vs* μ for 0.97 mm (LF) and 0.99 mm (HF) 2036-T4 aluminum on the 5.5 radius drawbead. The experimental curve for 0.99 (HF) material shows a slight deviation compared to the calculated curve toward lower drawing loads at higher μ. Differences between the curves at 0 friction and friction for MO lubricant are shown.

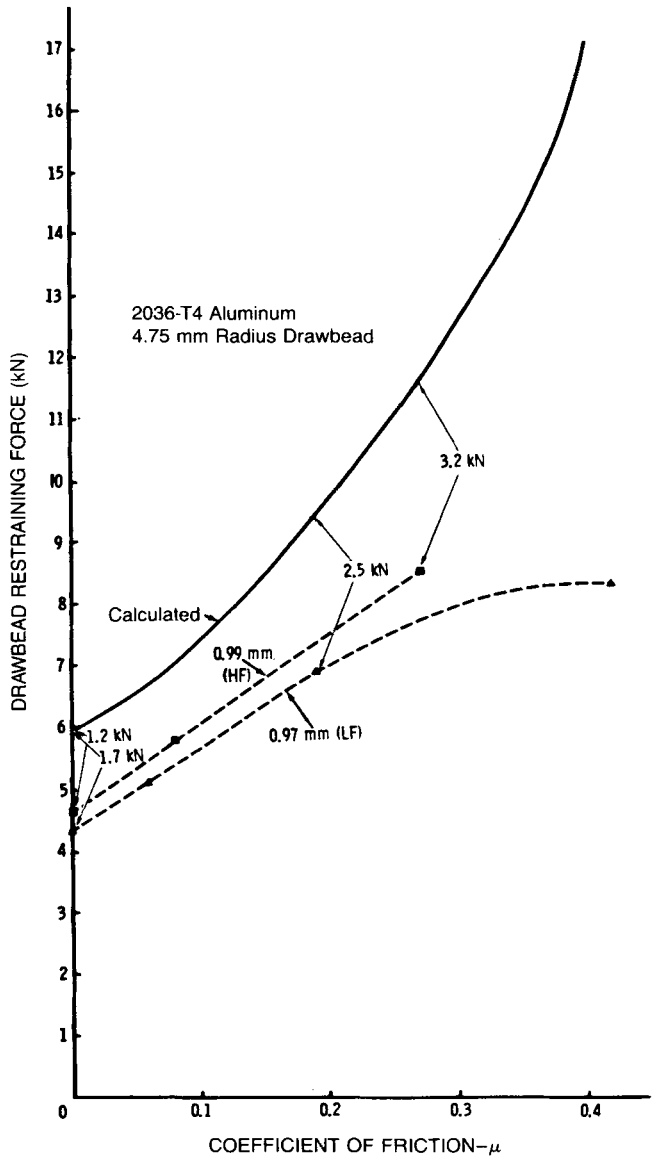

Fig. 10 — Drawbead Restraining force *vs* μ for 0.97 mm (LF) and 0.99 mm (HF) 2036-T4 aluminum on the 4.75 mm radius drawbead. The large divergence between experimental and calculated curves shows a breakdown in Coulomb's Law for friction in drawbeads. Differences between the curves at 0 friction and friction for MO lubricant are shown.

2036-T4 aluminum and is not a reasonable approximation to calculate the DR force.

CONCLUSIONS

1. The applicability of Coulomb's Law to drawbeads depends on complex interactions among the material, the contact pressure between the sheet metal and drawbead tool surfaces, the surface roughness, and the lubrication.
2. For rimmed and A-K steel, Coulomb's Law may be applied to drawbead friction for most autobody sheet thicknesses. For high contact pressures resulting from sheet thicknesses approaching 1 mm pulled through 4.75 mm radius drawbeads, a sudden increase in μ and burnishing of the drawbead surfaces indicates a change of lubrication regime and a breakdown of Coulomb's Law.
3. For 2036-T4 aluminum, Coulomb's Law applies to drawbeads for sheet thicknesses below about 0.9 mm. For thicknesses approaching 1 mm, poor lubrication conditions, and a relatively rough sheet metal surface, Coulomb's Law breaks down.

ACKNOWLEDGMENTS

The author appreciates the help of R. J. Dusman in designing the apparatus, and E. G. Brewer in setting up the measurements on the MTS testing machine. Neng-Ming Wang of the Mathematics Department contributed with many helpful discussions and together with Professor B. Budiansky, Harvard University, aided substantially in developing expressions for the coefficient of friction. W. F. Brazier, formerly at Fisher Body Division, made many helpful suggestions. T. Schreiber, A. Ottolini and H. Sturner of the Chemistry Department assisted with surface analysis and SEM photography. R. Lenz and C. Fox of the Engineering Mechanics Department made surface roughness measurements.

REFERENCES

1. H. D. Nine: *Mechanics of Sheet Metal Forming*, D. P. Koistinen and N.-M. Wang, eds., Plenum Press, 1978, p. 179.
2. W. R. D. Wilson: *Mechanics of Sheet Metal Forming*, D. P. Koistinen and N.-M. Wang, eds., Plenum Press, 1978, p. 157.
3. D. Tabor: *Proc. Roy. Soc. (London)*, 1959, vol. A251, p. 378–93.
4. R. C. Spragg and D. J. Whitehouse: *Proc. I. Mech. E.*, 1970, vol. 185, p. 697.
5. B. Fogg: *Sheet Metal Industries*, 1967, vol. 44, p. 478.
6. S. Fukui *et al.*: *Sheet Metal Industries*, 1963, vol. 40, p. 739.
7. B. Fogg: *Sheet Metal Industries*, 1976, vol. 53, p. 294–302, p. 304.
8. N. M. Wang: "A Mathematical Model of Drawbead Forces in Sheet Metal Forming," *Journal of Applied Metalworking*, July 1982, vol 2, no. 3, p. 193.